DOSE VERIFICATION IN RADIOTHERAPY OF PROSTATE CANCER PATIENTS WITH HIP PROSTHESIS*

B. Kiełtyka[a,†], K. Rawojć[b], R. Kopeć[c], J. Stanek[a]
A. Truszkiewicz[d,e], K. Kisielewicz[f]

[a]M. Smoluchowski Institute of Physics, Jagiellonian University, Kraków, Poland
[b]University Hospital in Kraków, Department of Endocrinology
Nuclear Medicine Unit, Poland
[c]H. Niewodniczański Institute of Nuclear Physics Polish Academy of Sciences
Kraków, Poland
[d]St. Jadwiga the Queen Clinical Hospital No. 2, Rzeszów, Poland
[e]Department of Photomedicine and Physical Chemistry, Faculty of Medicine
University of Rzeszów, Poland
[f]Centre of Oncology, Maria Skłodowska-Curie Memorial Institute
Kraków Branch, Poland

(Received May 7, 2020)

The main purpose of this paper was to evaluate radiation dose given to the patient, when they receive RT in the pelvic region and have hip prosthesis. All experiments were performed in the Center of Oncology, Maria Skłodowska-Curie Memorial Institute in Kraków. We used linac accelerators with the nominal energy of 6 MeV and 18 MeV in volumetric modulated arc therapy technique (VMAT). The treatment plans were calculated in the TPS with the application of anisotropic analytical algorithm (AAA). The goal of this study was to achieve a clinically acceptable dose distribution for PTV treated to 63 Gy (21 fx), so at least 98% of the PTV volume was covered with 95% isodose, with the maximum dose fixed on less than 107% of prescribed dose. Absorbed doses were evaluated by using thermoluminescent detectors. For lower energies, TPS overestimates the dose at the interface of significantly different density, while in the case of higher energies (18 MeV), the dose was underestimated. This underestimation, according to experimental data obtained previously, may reach, in the VMAT rotational dynamic technique, up to 13% in relation to data from TPS. Therefore, with the increasing number of patients with hip prosthesis treated for *i.e.* prostate cancer, it becomes crucial to carefully monitor the real doses and to keep doses below the risk limit.

DOI:10.5506/APhysPolBSupp.13.869

* Presented at the 45th Congress of Polish Physicists, Kraków, September 13–18, 2019.

† Corresponding author: bartosz.kieltyka@alumni.uj.edu.pl

1. Introduction

Modern treatment planning systems (TPS) use different types of dose calculation algorithms. The speed and quality of each TPS strongly varies between selected algorithms [1–3]. The accuracy of the dose prediction depends on the assumptions and approximations implemented in each algorithm. These approximations are the source of the administered dose uncertainty, especially in organs of high density gradient such as bone or lungs [4, 5]. The number of patients with a hip prosthesis who undergo pelvic radiation therapy is still increasing [6]. According to Task Group Report 63 (TG-63) of the American Association of Physics in Medicine (AAPM), around 4% of all patients undergoing radiation therapy (RT) have prosthetic inserts that can affect calculated dose. Most prostheses are produced using cobalt–chromium or titanium alloys. The corrosion resistance, fatigue resistance, mechanical strength, biocompatibility of these materials allow their application in prosthetics [7, 8]. Population aging and the increase in use of hip replacements generate a problem in accurate dose calculation [6], mostly due to the presence of materials with an electron density different from water. Therefore, there is a need for planning systems that should be tested and approved in various settings, especially for settings involving high atomic number material. In the case of patients with metal hip prosthesis, the treatment should be planned taking into account the material of the prosthesis, its location as well as geometrical design of photon beams. Due to interference with the radiation field and dose reduction to the tissue behind the prosthesis, the common practice is to avoid direct irradiation of the prosthesis material. There are two main challenges in RT planning for patients with bilateral or unilateral implants. One of them is generation of significant artifacts in computed tomography (CT) images what plays an important role in calculating the dose in RT [9, 10]. Second one is that the implant presence causes a significant weakening of the beam in the space behind it, which affects the dose distribution in the region (small pelvis, prostate). Besides, on the border of matters, there is a significant change in dose due to a radiation backscattering from the implant [11]. CT images are used in three-dimensional TPS. Applied CT is available in the state of providing information of the subject and its structural functions, their geometry in the use of the constraint function [12]. Artifacts generated by metal prosthesis contain significant computational errors in TPS [13]. TPS has certain limitations in modeling the production of charged particles and photon scattering with various materials [6, 14–20]. Dose miscalculation by the TPS potentially creates a threat to the tumor control and to the patient's life after the therapy [21]. Therefore, the main purpose of this paper was the evaluation of additional radiation dose given to the patient when irradiating regions with hip prosthesis.

2. Materials and methods

All experiments were performed in the Center of Oncology, Maria Skłodowska-Curie Memorial Institute in Kraków. We used linac accelerators Unique and Truebeam, Varian Medical Systems in the energy range of 6 MeV and 18 MeV in volumetric modulated arc therapy technique (VMAT). The treatment plans were calculated in the TPS ECLIPSE, ver. 11 with the application of anisotropic analytical algorithm ver. 11.0.31 (AAA).

The main goal of this study was to achieve a clinically acceptable dose distribution for PTV treated to 63 Gy (21 fx), so at least 98% of the PTV volume was covered with 95% isodose, with the maximum dose fixed on less than 107% of prescribed dose. The dose in organs at risk (OAR) (rectum, posterior rectal wall and bladder) has been minimized to meet the DVH criteria. Absorbed doses were evaluated by using thermoluminescent detectors (TLDs) read at the Institute of Nuclear Physics Polish Academy of Sciences, Bronowice Cyclotron Center.

The AAA is based on semianalytic mathematical model. The AAA core is estimated on pencil beams which are determined on the Monte Carlo simulations tailored to user-supplied beam measurements. These beams are then used as a multi-sourced model. Heterogeneity correction of AAA to some extent takes into account scattered radiation from the computational environment *i.e.* lateral scaling of the medium uses six independent exponential functions including lateral energy transport with variable densities [22–24]. AAA reports the doses as Dw, m with the corrections estimated on the electron density applied to the dose core calculated in water [25–27].

In order to verify the dose at the border between the bone and endoprosthesis, a specially designed phantom was built. The phantom shape was corresponding to the human pelvis and installed there endoprosthesis — hip joint, acetabulum with the head and femoral neck [28].

An artificial pelvis was made of plastic — PVC — with HU 1300–1500 value, according to data obtained from a CT scanner. Phantom material was free from defects that accompanied previously selected materials such as dried human bone (from the archaeological resources of the Jagiellonian University) or pork bone, which were characterized by inadequate density and/or the inability to reuse due to material deterioration. Moreover, PVC was relatively easy to process and TLDs application was quick and repeatable, in contrast to animal bones.

The Aesculap endoprostaesis, Screw Socket S.C. was used for the study. The NH448T with 48 mm diameter ISOTANF alloy type (Ti_6Al_4V/ISO 5832-3). This alloy is used in bone surgery in a two-phase $\alpha + \beta$ structure also known under the trade name Prorasul — 64WF. A cement-free mandrel was also used (Aesculap — NC087K — ISODUR — alloy type (CoCrMo/ISO 5832-12).

The phantom, the tripod holding pelvis and the endoprosthesis placed in a repetitive position, were used for irradiation. The phantom was entirely created from tissue-like material (PMMA), commonly used in both radiotherapy and radiology Its interior was filled with water. The lateral dimensions of the phantom were comparable to that of the adult male pelvis. The isocenter was at the center of the phantom.

TLDs-type MTS-N were placed in previously prepared cavities, after assembling all phantom elements, on the surface connecting the prosthesis with the bone [29, 30]. 64 detectors with a diameter of $\phi = 4.5$ mm, thickness of $d = 0.7$ mm and a mass of $m = 35\,\text{mg} \pm 0.5\,\text{mg}$ were applied at once, then were used to verify the actual dose deposited in the bone tissue at the border centers [31, 32]. In order to protect the detectors against falling out, they were glued with kapton tape slightly contaminating the surface of the detectors. After the irradiation process was completed, the dose was read using a Lexygsmart TL/OLS reader. Dose calibration was performed for each batch of detectors (for 2 Gy, 1 Gy, 0.5 Gy, and for the background dose) on the apparatus, on which the phantom measurements were performed. The background dose has been minimized by TLD annealing just before reading.

3. Results

Obtained results that were carried out, determined and read from the TPS were presented in the form of graphs. After processing we presented the data as histograms containing information about the number of nests (places of reading and the dose deposition), depending on the difference in the dose from TPS and real dose accumulated in a given anatomical area for both energies — 6 MeV and 18 MeV of photons.

For radiation with a nominal energy of 6 MeV, 8 series of irradiations were carried out, in which 512 TLD detectors were irradiated (in total 32 detectors used for one dose calibration). At each series, the detectors were numbered and embedded in specially prepared nests in the pelvic bone. Then for a given nest, the dose was averaged over all experimental series and compared with the result obtained from TPS (presented in figures below). After adjusting the normal distribution to the obtained differential histogram for individual nest, the average value of the dose difference was: $\text{MeanNormal} = 0.109 \pm 0.097$ [Gy]. As a result of irradiation in rotational dynamic VMAT technique, this gives a result by 9.83% lower in the area located on the border of the centers of bone tissue–prosthesis compared to the value predicted by the TPS.

For the nominal energy of 18 MeV, 6 series of irradiations were performed for 384 TLD detectors and 32 detectors used for the dose calibration. As in the case of detectors used for 6 MeV radiation, here, the same detectors were properly numbered to identify the location of the place where the ionizing radiation dose verification was carried out. Similarly to previous sessions, a differential histogram was prepared for individual nests and the average value of the difference in dose was: MeanNormal $= -0.1447 \pm 0.081$ [Gy]. This result, in a relation to the average dose value calculated by the TPS for individual nests, was 12.75% higher.

We observed that the detectors located in the center of the acetabulum received a higher dose compared to the detectors located on the edge of the acetabulum. This tendency is noticeable both in the case of lower energy 6 MeV of radiation used and in the case of higher energy 18 MeV, and presented in Figs. 1 and 2.

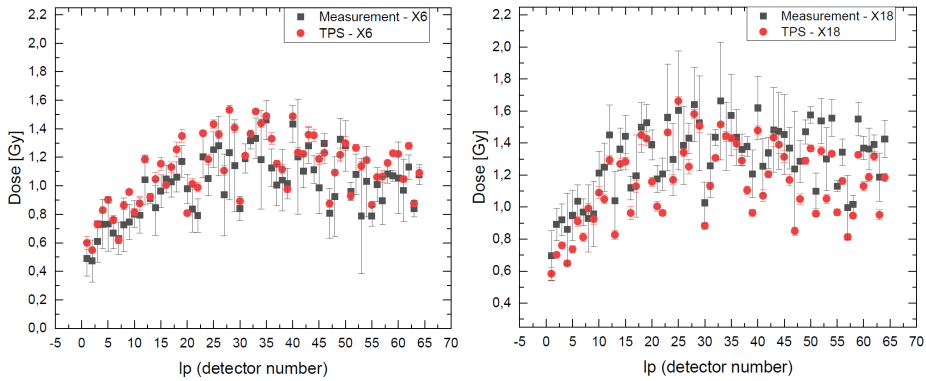

Fig. 1. The comparison of the mean dose measured by TLDs for both nominal energies: 6 and 18 MeV of photons.

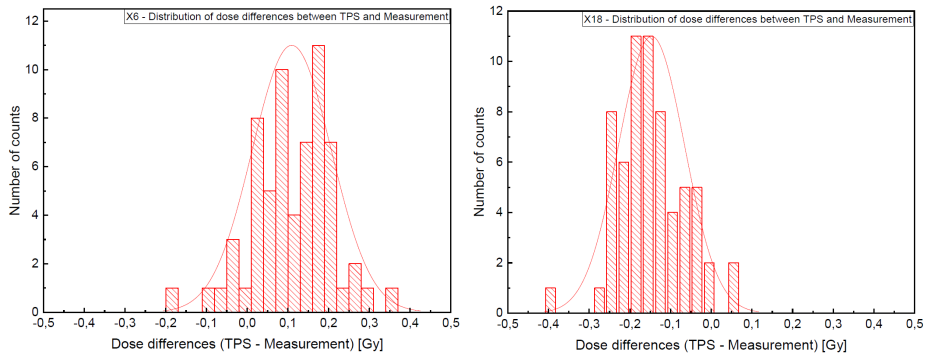

Fig. 2. Histograms presenting the difference in the dose calculated by TPS and real dose measured by TLDs for both used nominal energies: 6 and 18 MeV of photons.

4. Discussion

Nowadays, the number of patients with a hip prosthesis undergoing pelvic radiation therapy is increasing [6]. According to Task Group Report 63 (TG-63) of the American Association of Physics in Medicine (AAPM), between 1% and 4% of patients receiving radiation therapy have prosthetic devices that may affect the calculated dose. The high atomic number and density of implants lead to serious problems in insuring accurate dose distribution in radiation therapy not only due to increased uncertainty in dose calculations in structures adjacent to these prosthesis, but also because the contouring of tumors and organs at risk is affected by artifacts in CT scans (AAPM-85 report) [33].

Due to the use of high-energy ionizing radiation during the treatment of patients, the TPS algorithms limitations may lead to serious errors in the dose calculation, which subsequently delivered during the therapy session may change significantly, when compared to the dose calculation originally assumed [34, 35]. This in turn might have a highly adverse effect on the patient's treatment results [36, 37]. As shown by the experiment carried out for the purposes of this work, this type of change is significant and reaches up to 10% for lower value (compared to planned by TPS, using the AAA) when it comes to commonly used energies (6 MeV) in dynamic techniques.

Furthermore, for lower energies, we observed that TPS overestimates the dose at the interface of significantly different density, while in the case of higher energies (18 MeV), the dose was underestimated. This underestimation, according to experimental data obtained previously, may reach, in the VMAT rotational dynamic technique, up to 13% in relation to data from TPS. The discrepancy between the experimental results and those obtained from the calculations of algorithms implemented into the TPS is associated with a phenomena to which high-energy ionizing radiation used for radiation therapy is subjected. These include: hardening of the beam by a high-density metal element, beam strong weakening, loss of electron balance, as well as radiation scattering and neutron production.

All these factors affect the cumulative dose in tissues on the border of the materials. The change in dose value in relation to the predictions of commonly used dose calculation algorithms can reach even more than 20% according to the Monte Carlo simulation [6, 13, 36, 38] resulting in both underestimation or overestimation. Such a large change in the primary beam arising from the interaction with high atomic number (Z) material might cause complications in both soft and hard tissues around the implant. These complications include skeletal changes (leading to hip fractures) or even necrosis or weakening of implant fixation.

An excess dose to the bone surrounding high atomic number (Z) material may have long-term consequences, including necrosis, bone weakness, and potential failure of the prosthetic device. Avoiding these complications may become an important factor in planning procedures in the vicinity of materials with a high-Z number. The work of other groups indicates incorrect dose determination near the prosthesis by treatment planning algorithms which is in agreement with the observation. The paper presents measurements of the patient's pelvis imitating phantom and two beam energies commonly used in radiotherapy

The size of the dose calculation grid must be as small as possible to correctly calculate sharp dose gradients at the high-Z tissue/material boundaries. The size of prosthesis will affect the fluence transmission. It may also affect the amount of dose at points behind the prosthesis, but will not affect the dose due to the backscattering.

With the increasing number of patients with hip prosthesis treated for prostate cancer, it becomes crucial to carefully monitor the real doses and to keep doses below the risk limit. Additional follow up with monitored absorbed doses should be provided. Oncologist and medical physicist would have an electronic database of doses prescribed and measured on-site. These parameters may be most important when the disease relapse in the same region and further radiation therapy will be needed.

REFERENCES

[1] L.S. Constine *et al.*, «Late Effects of Cancer Treatment on Normal Tissues», in: E.C. Halperin, C.A. Perez, L.W. Brady, D.E. Wazer, C. Freeman, L.R. Prosnitz (Eds.) «Perez and Brady's Principles and Practice of Radiation Oncology», *Lippincott Williams & Wilkins*, Philadelphia, Pa 2008, pp. 320–355, 5$^{\text{th}}$ ed.

[2] M.K. Bucci *et al.*, *CA Cancer J. Clin.* **55**, 117 (2005).

[3] Animesh, *J. Cancer Res. Ther.* **1**, 12 (2005).

[4] J.R. Butts, A.E. Foster, *J. Appl. Clin. Med. Phys.* **2**, 32 (2001).

[5] M.H. Lin *et al.*, *Phys. Med. Biol.* **58**, 1027 (2013).

[6] C. Reft *et al.*, *Med. Phys.* **30**, 1162 (2003).

[7] M. Semilitsch, H.G. Willert, *Med. Biol. Eng. Comput.* **18**, 511 (1980).

[8] M. Tatcher, S. Palti, *Radiology* **141**, 201 (1981).

[9] C. Coolens, P.J. Childs, *Phys. Med. Biol.* **48**, 1591 (2003).

[10] C. Glide-Hurst *et al.*, *Med. Phys.* **40**, 061711 (2013).

[11] E. Buffard *et al.*, *Nucl. Instrum. Methods Phys. Res. B* **251**, 9 (2006).

[12] G.X. Ding, C.W. Yu, *Int. J. Radiat. Oncol. Biol. Phys.* **51**, 1167 (2001).

[13] S.Y. Lin *et al.*, *Appl. Radiat. Isot.* **57**, 17 (2002).

[14] P.J. Keall *et al.*, *Med. Dosim.* **28**, 107 (2003).
[15] M. Carolan *et al.*, *Australas. Radiol.* **44**, 290 (2000).
[16] M. Erlanson *et al.*, *Int. J. Radiat. Oncol. Biol. Phys.* **20**, 1093 (1991).
[17] W.D. Burleson *et al.*, *Int. J. Radiat. Oncol. Biol. Phys.* **20**, 1347 (1991).
[18] J.H. Kung *et al.*, *Med. Dosim.* **26**, 305 (2001).
[19] W.U. Laub, F. Nüsslin, *Med. Dosim.* **28**, 229 (2003).
[20] R. Roberts, *Phys. Med. Biol.* **46**, N227 (2001).
[21] G.G. Alves *et al.*, *Braz. J. Med. Biol. Res.* **48**, 644 (2015).
[22] W. Ulmer, D. Harder, *Z. Med. Phys.* **5**, 25 (1995).
[23] W. Ulmer, D. Harder, *Z. Med. Phys.* **6**, 68 (1996).
[24] W. Ulmer *et al.*, *Phys. Med. Biol.* **50**, 1767 (2005).
[25] G.A. Failla *et al.*, «Acuros XB Advanced Dose Calculation for the Eclipse Treatment Planning System», *Varian Medical Systems*, Palo Alto, CA 2010.
[26] O.N. Vassiliev *et al.*, *Phys. Med. Biol.* **55**, 581 (2010).
[27] T. Han *et al.*, *Med. Phys.* **38**, 2651 (2011).
[28] B. Kiełtyka *et al.*, *Acta Phys. Pol. B* **51**, 263 (2020).
[29] B. Obryk, «Raport Nr. 2045/D — Opracowanie metody pomiaru wysokich dawek promieniowania jonizującego z zastosowaniem wysokoczułych detektorów termoluminescencyjnych LiF:Mg, Cu, P», http://www.ifj.edu.pl/badania/publikacje/raporty/2010/2045.pdf?lang=pl, Kraków, 2010, (in Polish).
[30] B. Obryk, P. Bilski, «Thermoluminescent dosimetry service at the IFJ Kraków», Seminarium RADMON (Radiation Monitoring Working Group at CERN), http://indico.cern.ch/conferenceDisplay.py?confId=12735, 2007.
[31] P. Wesolowska *et al.*, *Acta Oncol.* **58**, 1731 (2019).
[32] K. Chełmiński, W. Bulski, *Rep. Pract. Oncol. Radiother.* **15**, 40 (2010).
[33] «Tissue inhomogeneity corrections for megavoltage photon beams», report No. AAPM-85 of Task Group No. 65 of the Radiation Therapy Committee of the American Association of Physicists in Medicine, Madison, WI: Medical Physics Publishing; 2004, DOI: https://doi.org/10.37206/86
[34] A. Mesbahi, F.S. Nejad, *Radiat. Med.* **25**, 529 (2007).
[35] K. Mohammadi *et al.*, *J. Cancer Res. Ther.* **13**, 501 (2017).
[36] S.Çatlı, G. Tanır, *Med. Dosim.* **38**, 332 (2013).
[37] S. Spirydovich *et al.*, *Radiother. Oncol.* **81**, 309 (2006).
[38] C. Paulu, P. Alaei, *J. Appl. Clin. Med. Phys.* **18**, 9 (2017).